Numerical Solution for the Scattering of Sound Waves by a Circular Cylinder

R.T. Ling*
Northrop Aircraft Division, Hawthorne, California

A numerical method is presented for the solution of the scattering of sound waves by a long circular cylinder. A generalized scattering amplitude is introduced and used to derive a transformed Helmholtz equation. Coupled with radiation condition and cylinder surface boundary conditions, the transformed Helmholtz equation is solved by a finite-difference method. Numerical results for both acoustically soft and hard cylinders are obtained for $ka \leq 12$, where k is the wave number equaling 2π divided by the wavelength of the sound waves and a is the radius of the cylinder. These results are in excellent agreement with those obtained by the eigenfunction expansion method. Results presented include spatial profiles of the generalized scattering amplitude, amplitude and phase of the total wave, and bistatic scattering cross sections. The dependence of the total scattering cross section on ka is tabulated. The optical theorem is satisfied to within 3% error in most cases. The method shows promise for accurate, systematic calculations for bodies of arbitrary material, size, and shape.

I. Introduction

THE Helmholtz equation that arises from Euler's equation and mass continuity equation can be solved by differential equation and integral equation methods. One of the differential equation methods[1-3] involves separation of variables in specific coordinate systems. The solution is written as an infinite series of eigenfunctions of the separated operators. This method is applicable only for a few simple obstacle geometries such as a circular cylinder or a sphere. In recent years, there have been attempts[4-6] to solve the Helmholtz equation directly for scalar scattering problems by finite-difference methods. However, due to the infinite extent of physical space and the oscillatory nature of field quantities, a large number of grid points are needed for accurate solutions with such an approach. Convergence of numerical solutions and enforcement of radiation conditions present serious difficulties in this direct solution method. Although a preconditioned conjugate gradient iterative method[5] has been proposed to alleviate the convergence problems, and various schemes[4,6] have been proposed to enforce the radiation condition at a finite distance from the obstacle, the direct solution method does not seem practical for scattering problems. The integral equation method[7,8] involves solving a Fredholm equation of the second kind over the surface of the scatterer. The integral equations are difficult to solve, though principles of physical optics can be used to simplify the equations in the short wavelength limit.

The numerical method presented in this paper follows the differential equation approach, but it differs from both the eigenfunction expansion method and the direct solution of the total wave method. In this approach, the asymptotic form of the scattered wave, represented as outgoing spherical or cylindrical waves modulating a scattering amplitude, is extended inward throughout the scattering region by defining a generalized scattering amplitude that depends not only on the scattering angle but also on the radial distance from the scattering center. The generalized scattering amplitude, though it may vary with radial distance, would be mainly nonoscillatory and approach asymptotically the ordinary scattering amplitude as its limiting value. The scattered wave remains oscillatory due to the modulating outgoing wave. The total wave is also oscillatory as a result of the interference between the incident plane wave and the scattered wave.

The concept of the generalized scattering amplitude is analogous to that of the wave envelope[9] used in various studies of sound propagation in ducts. This wave envelope concept was shown to reduce significantly (by two orders of magnitude) the number of grid points required for steady-state solution of high-frequency sound propagation in ducts. The reduction was possible due to the nonoscillatory nature of the wave envelope. A time-dependent numerical method[10] has also been developed to further reduce the computer storage and run times.

The governing differential equation in terms of the generalized scattering amplitude can be readily derived from the Helmholtz equation. The transformed Helmholtz equation with the corresponding radiation condition and surface boundary conditions can be solved by the finite-difference method. The nonoscillatory nature of the generalized scattering amplitude and its asymptotic behavior allow one to map the infinite physical space onto a finite computational space on which a relatively crude grid network can be used to obtain an accurate solution. The body surface boundary conditions and the far-field radiation condition at infinity can be enforced exactly. Thus, the numerical difficulties encountered in the direct solution of the total wave from the original Helmholtz equation are avoided.

II. Differential Equation Formulation for the Generalized Scattering Amplitude

The problem under consideration is that of a plane wave incident normally on an infinitely long circular cylinder. The schematics of the scattering problem and the cylindrical coordinate system are illustrated in Fig. 1. The incident sound wave of wavelength λ and frequency ν propagates in the positive x axis direction and is represented by $\exp[i(kx-wt)]$, where $k=2\pi/\lambda$ is the wavenumber and $w=2\pi\nu$ is the angular frequency. The axis of the cylinder lies along the z axis, and the cylinder radius is denoted by a.

The propagation of sound in an inviscid fluid at rest can be described by the variation of fluid pressure or fluid particle velocity that can be expressed as the gradient of a scalar

Received April 30, 1986; presented as Paper 86-1880 at the AIAA 10th Aeroacoustics Conference, Seattle, WA, July 9-11, 1986; revision received Sept. 2, 1986.

*Engineering Specialist. Member AIAA.

potential. Combining Euler's equation and the mass continuity equation, a wave equation is obtained that is satisfied by both the excess pressure (i.e., the difference between the actual pressure and the pressure of the fluid at rest) and the velocity potential:

$$\nabla^2\phi = \frac{1}{c^2}\frac{\partial^2\phi}{\partial t^2} \tag{1}$$

where ϕ is either the excess pressure or the velocity potential, and $c=\lambda\nu=w/k$ is the speed of sound in the fluid. An exp $[-iwt]$ time dependence is assumed for the fluid excess pressure and the particle velocity. This harmonic time dependence is suppressed throughout the consideration. The wave equation, Eq. (1), then reduces to the scalar Helmholtz equation

$$\nabla^2\phi + k^2\phi = 0 \tag{2}$$

In cylindrical coordinates, it assumes the form

$$\frac{\partial^2\phi}{\partial r^2}+\frac{1}{r}\frac{\partial\phi}{\partial r}+\frac{1}{r^2}\frac{\partial^2\phi}{\partial\theta^2}+k^2\phi=0 \tag{3}$$

where we have used the symmetry property in eliminating the z dependence of the excess pressure and the velocity potential. Since the excess pressure vanishes on the surface of an acoustically soft cylinder and the fluid particle velocity vanishes on the surface of an acoustically hard cylinder, the corresponding boundary conditions are

$$\phi(a,\theta)=0 \tag{4a}$$

a Dirichlet condition for an acoustically soft cylinder, and

$$\left(\frac{\partial\phi}{\partial r}\right)_{r=a}=0 \tag{4b}$$

a Neumann condition for an acoustically hard cylinder.

The total wave ϕ can be represented as a superposition of an incident wave ϕ^i and a scattered wave ϕ^s, $\phi=\phi^i+\phi^s$. In the far field, the radiation condition applies to the scattered wave,

$$\lim_{r\to\infty}\sqrt{r}\left(\frac{\partial}{\partial r}-ik\right)\phi^s=0 \tag{5}$$

The Helmholtz equation, Eq. (3), together with the body surface boundary condition, Eq. (4a) or (4b), and the radiation condition, Eq. (5), define the scattering problem mathematically.

To avoid dealing with the oscillations in the total and scattered waves in the infinite extent of physical space, we reformulate the scattering problem in terms of a nonoscillatory generalized scattering amplitude that approaches the ordinary scattering amplitude asymptotically in the far field. In this approach, the total wave is written in the following form:

$$\phi=e^{ikx}+f(r,\theta)\frac{e^{ikr}}{\sqrt{kr}} \tag{6}$$

where $f(r,\theta)$ is the generalized scattering amplitude. Substitution of Eq. (6) into Eq. (3) results in a transformed Helmholtz equation

$$\frac{\partial^2 f}{\partial r^2}+2ik\frac{\partial f}{\partial r}+\frac{1}{r^2}\frac{\partial^2 f}{\partial\theta^2}+\frac{1}{4}\frac{1}{r^2}f=0 \tag{7}$$

The unknown function f is a complex function whose real and imaginary parts are coupled through the $2ik(\partial f/\partial r)$ term in Eq. (7). Substituting the second term on the right-hand side of Eq. (6) into the radiation condition, Eq. (5), we obtain

$$\lim_{r\to\infty}\frac{\partial f(r,\theta)}{\partial r}=0 \tag{8}$$

a very simple Neumann condition on the far-field boundary. This condition is expected since the generalized scattering amplitude has no radial distance dependence in the far field. The body surface boundary conditions in terms of $f(r,\theta)$ corresponding to Eqs. (4a) and (4b) can be readily obtained by substituting Eq. (6) into Eqs. (4a) and (4b). Thus they become

$$f(a,\theta)=g(\theta) \tag{9a}$$

a Dirichlet condition, and

$$\alpha(\theta)f(a,\theta)+\beta(\theta)\left(\frac{\partial f}{\partial r}\right)_{r=a}+\gamma(\theta)=0 \tag{9b}$$

a mixed condition. In Eqs. (9a) and (9b), $g(\theta)$, $\alpha(\theta)$, $\beta(\theta)$, and $\gamma(\theta)$ are known functions of the azimuthal angle. These transformed body surface boundary conditions, Eqs. (9a) or (9b), together with the transformed radiation condition, Eq. (8), and with the transformed Helmholtz equation, Eq. (7), define a well-posed elliptic problem equivalent to the original one defined by Eqs. (2), (4), and (5). A unique, stable solution exists.

The solution of the generalized scattering amplitude over the physical range of r and θ completely determines the scattered wave. Of particular interest is the angular dependence of the intensity of the scattered wave at infinity. In the case of normal incidence on an infinitely long cylinder, the bistatic acoustic scattering cross section per unit cylinder length $\sigma(\theta)$ can be defined in a manner similar to the definition of bistatic

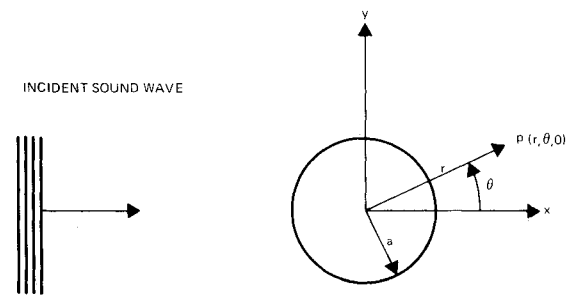

Fig. 1a Normal incidence of a plane sound wave on a circular cylinder.

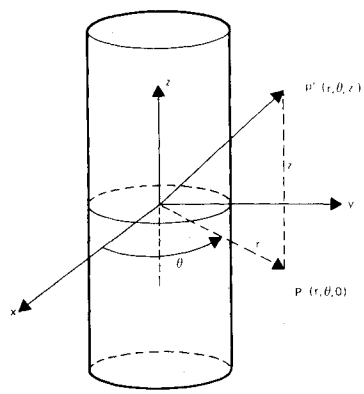

Fig. 1b Cylindrical coordinate system.

radar cross section in electromagnetic wave scattering

$$\sigma(\theta)=\lim_{r\to\infty} 2\pi r\frac{|\phi^s|^2}{|\phi^i|^2} \tag{10}$$

where ϕ^s is the scattered wave, and ϕ^i is the incident plane wave. For the unit amplitude plane wave e^{ikx} in Eq. (6), it follows that

$$\sigma(\theta)=\frac{2\pi}{k}|f(\infty,\theta)|^2 \tag{11}$$

The total acoustic scattering cross section per unit length σ_T is defined as the average of the bistatic acoustic scattering cross sections per unit length over the entire range of scattering angles. Therefore, we have

$$\sigma_T=\frac{1}{k}\int_0^{2\pi}|f(\infty,\theta)|^2 d\theta=\frac{1}{2\pi}\int_0^{2\pi}\sigma(\theta)d\theta \tag{12}$$

A relationship between the total scattering cross section and the scattering amplitude in the forward direction, known as the optical theorem or the forward scattering theorem[3], can be derived as a consequence of conservation of energy flux. For the particular form of the scattered wave given in Eq. (6), it can be shown that

$$\sigma_T=(\sqrt{4\pi}/k)[f^i(\infty,0)-f^r(\infty,0)] \tag{13}$$

where $f^r(\infty,0)$ and $f^i(\infty,0)$ are the real and imaginary parts of the asymptotic scattering amplitude in the forward direction. Since the total scattering cross section can also be found by integrating the bistatic cross sections over the range $0\le\theta\le 2\pi$, according to Eq. (12); the optical theorem, Eq. (13), serves as a check on the accuracy of numerical solutions.

III. Finite-Difference Technique

The transformed Helmholtz equation and boundary conditions for the generalized scattering amplitude can be solved by a finite-difference method. The nonoscillatory, smoothly varying behavior of the generalized scattering amplitude allows one to make suitable coordinate transformations to map the infinite physical domain onto a finite computational domain. Tangent and inverse hyperbolic tangent functions are examples of suitable coordinate transformations,

$$r=a+c_1\tan(\frac{\pi}{2}\eta) \tag{14}$$

$$r=a+c_2\tanh^{-1}(\eta) \tag{15}$$

where one can adjust the constants c_1 and c_2 to control the stretching of the grid points in the physical space. Both transformations map the infinite range $a\le r\le\infty$ of the radial distance in the physical space onto the finite range $0\le\eta\le 1$ of the transformed radial coordinate in the computational space. These two coordinate transformations provide densely packed grid points near the cylinder surface to resolve the expected high gradients in the generalized scattering amplitude in this region.

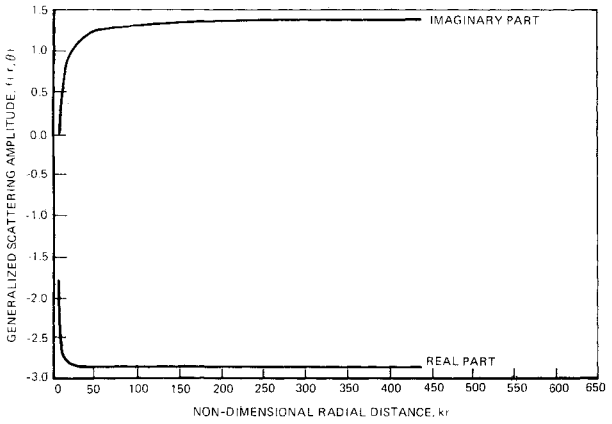

Fig. 2 Generalized scattering amplitude profile; soft cylinder, $ka=3.1$, $\theta=0$.

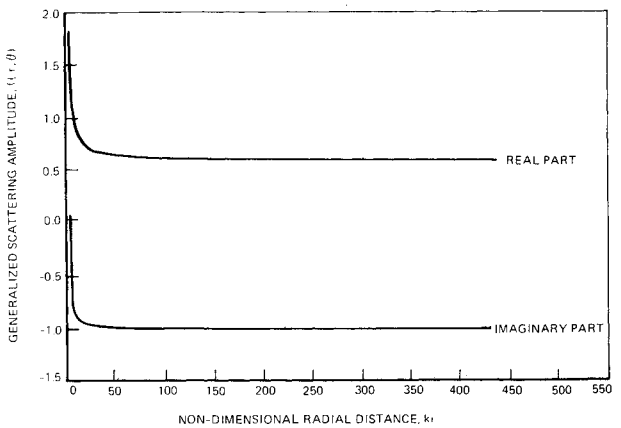

Fig. 3 Generalized scattering amplitude profile; soft cylinder, $ka=3.1$, $\theta=\pi/2$.

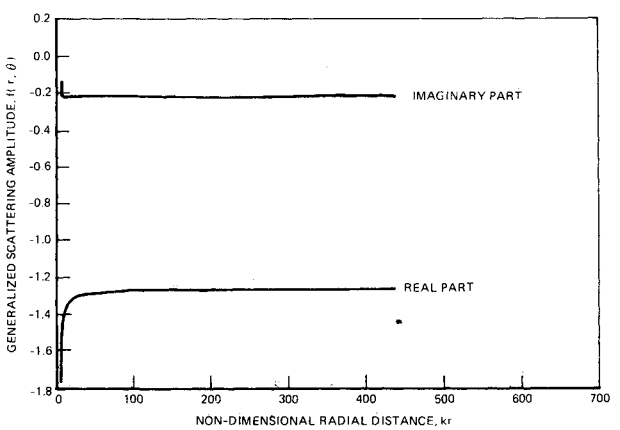

Fig. 4 Generalized scattering amplitude profile; soft cylinder, $ka=3.1$, $\theta=\pi$.

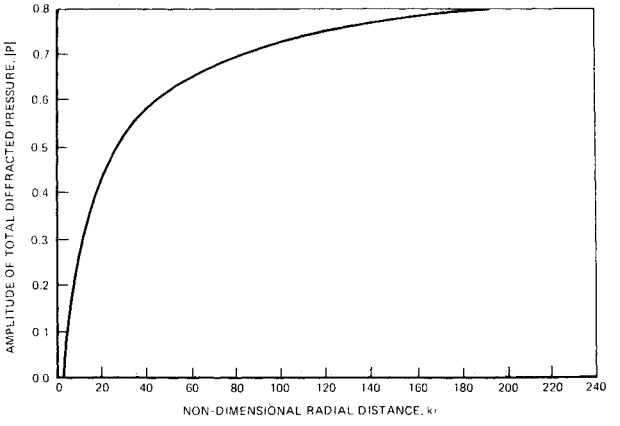

Fig. 5 Amplitude of total diffracted pressure field; soft cylinder, $ka=3.1$, $\theta=0$.

Under the coordinate transformation $r=r(\eta)$, the transformed Helmholtz equation, Eq. (7), becomes

$$t^2\frac{\partial^2 f^r}{\partial\eta^2}+u\frac{\partial f^r}{\partial\eta}+v\frac{\partial^2 f^r}{\partial\theta^2}+\frac{v}{4}f^r=2kt\left(\frac{\partial f^i}{\partial\eta}\right) \tag{16a}$$

$$t^2\frac{\partial^2 f^i}{\partial\eta^2}+u\frac{\partial f^i}{\partial\eta}+v\frac{\partial^2 f^i}{\partial\theta^2}+\frac{v}{4}f^i=-2kt\left(\frac{\partial f^r}{\partial\eta}\right) \tag{16b}$$

where f^r and f^i are the real and imaginary parts of the generalized scattering amplitude and

$$t=\frac{\partial\eta}{\partial r},\qquad u=\frac{\partial^2\eta}{\partial r^2},\qquad v=\frac{1}{r^2} \tag{17}$$

For the normal incidence on a circular cylinder, the total and scattered waves are symmetric with respect to the x axis, $f(r,-\theta)=f(r,\theta)$ for all θ. A uniform grid network is placed on the finite computational domain $0\le\theta\le\pi$ and $0\le\eta\le 1$. Second-order-accurate, centered finite-difference expressions are used to translate Eq. (16) into a set of simultaneous linear algebraic equations. The boundary conditions, Eqs. (8) and (9), are enforced using second-order-accurate, one-sided finite-difference expressions for the first-order derivatives. The central-difference expressions used for the interior points are given by

$$\frac{\partial^2 f}{\partial\eta^2}=\frac{f_{i-1,j}-2f_{i,j}+f_{i+1,j}}{\Delta\eta^2} \tag{18a}$$

$$\frac{\partial f}{\partial\eta}=\frac{f_{i+1,j}-f_{i-1,j}}{2\Delta\eta} \tag{18b}$$

$$\frac{\partial^2 f}{\partial\theta^2}=\frac{f_{i,j-1}-2f_{i,j}+f_{i,j+1}}{\Delta\theta^2} \tag{18c}$$

where subscripts i and j denote the space indices and where $\Delta\eta$ and $\Delta\theta$ are the grid spacings. The backward-difference formula

$$\frac{\partial f}{\partial\eta}=\frac{f_{i-2,j}-4f_{i-1,j}+3f_{i,j}}{2\Delta\eta} \tag{19a}$$

is used for the radiation condition, while the forward-difference formula

$$\frac{\partial f}{\partial\eta}=\frac{-f_{i+2,j}+4f_{i+1,j}-3f_{i,j}}{2\Delta\eta} \tag{19b}$$

is used for the first-order derivative in the surface boundary condition. The simultaneous linear algebraic equations with boundary conditions properly enforced are solved by direct inversion of the associated matrix.

IV. Numerical Results and Discussions

For a plane wave normally incident on an infinitely long circular cylinder, the eigenfunction expansion method has been used by King and Wu[2] and by Bowman, Senior, and Uslenghi[3] to compute the amplitude and phase of the total and scattered

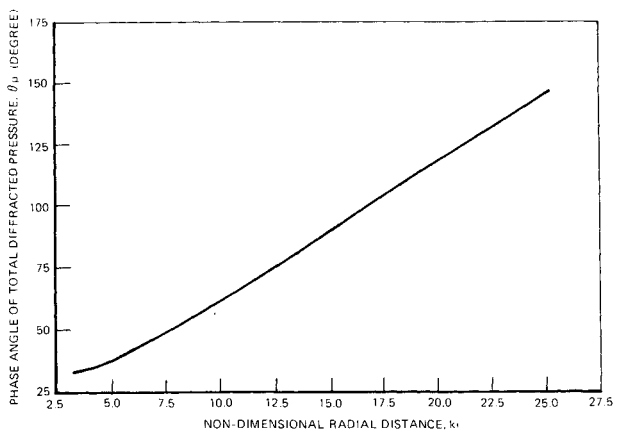

Fig. 6 Phase of total diffracted pressure field; soft cylinder, $ka=3.1$, $\theta=0$.

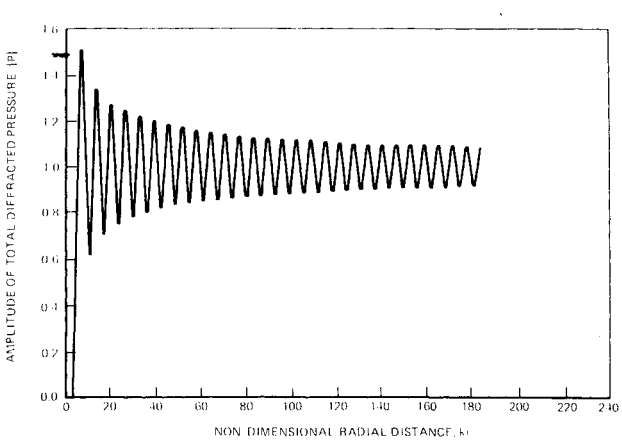

Fig. 7 Amplitude of total diffracted pressure field; soft cylinder, $ka=3.1$, $\theta=\pi/2$.

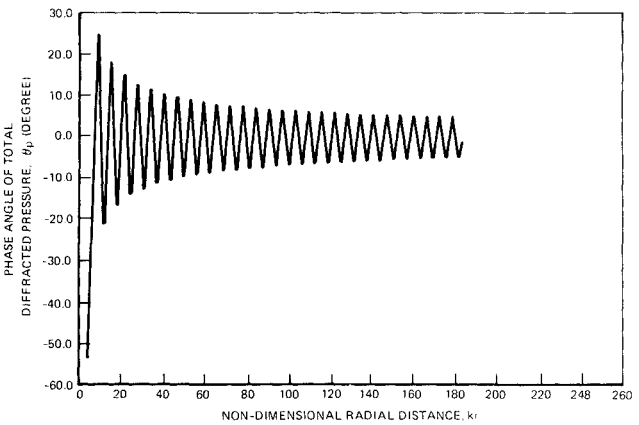

Fig. 8 Phase of total diffracted pressure field; soft cylinder, $ka=3.1$, $\theta=\pi/2$.

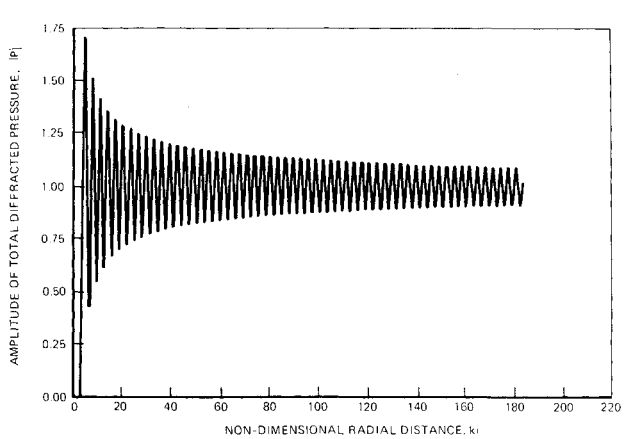

Fig. 9 Amplitude of total diffracted pressure field; soft cylinder, $ka=3.1$, $\theta=\pi$.

waves for various ka values at several locations in the scattering region. These authors considered a mathematically equivalent problem of a plane electromagnetic wave normally incident on an infinitely long, perfectly conducting circular cylinder. Due to the identical governing differential equation and boundary conditions, the scattering of sound waves by an acoustically soft cylinder is mathematically equivalent to the scattering of electromagnetic waves by a perfectly conducting cylinder for the polarization case in which the incident electric field is parallel to the cylinder axis. Similarly, the scattering of sound waves by an acoustically hard cylinder is mathematically equivalent to the scattering of electromagnetic waves by a perfectly conducting cylinder for the polarization case in which the incident magnetic field is parallel to the cylinder axis. Morse[1] provided the intensity of the scattered wave at $ka = 1$, 3, and 5 for scattering by a rigid (hard) cylinder. In this section, we present solutions based on the approach outlined in Secs. II and III and compare them with the results from the eigenfunction expansion method.

Soft-Cylinder Scattering

For the scattering by a soft cylinder at $ka = 3.1$, profiles of the generalized scattering amplitude are shown in Figs. 2-4 for scatterings in the forward, perpendicular, and backscattering directions. The real and imaginary parts of the generalized scattering amplitude show rapid changes within a few wavelengths of the cylinder's surface. This rapid variation in the generalized scattering amplitude is due to strong interactions between the incident sound waves and the obstacle and is confined to a small region near the obstacle. Outside the strong interaction region is an asymptotic region where the generalized scattering amplitude varies slowly and approaches its far-field limiting value. The size and shape of the strong interaction region depend on the cross-sectional shape of the cylinder and the wavelength of the incident plane wave. The existence of the asymptotic region is dictated by the radiation condition that requires the scattered wave to be a radially outgoing cylindrical wave modulating an amplitude function that at sufficiently large distances from the scattering center has vanishing dependence on the radial distance. Figures 5-10 show the amplitude and phase of the total sound pressure computed from Eq. (6). The amplitudes of the total waves are normalized to the incident wave amplitude, which is taken to be unity. The behavior of the total wave can be explained as a result of the interference between the incident wave and the scattered wave. In the forward direction, the incident wave and the scattered wave are in phase with each other. It results in no oscillation (Fig. 5) in the amplitude of the total wave. In the backscattering direction, incident and scattered waves are 180 deg out of phase, and it results in the most rapid oscillations (Fig. 9) in the total wave amplitude. Between these two extremes, the oscillation in the amplitude of the total wave increases from the forward to backscattering directions. Figures 6 and 10 show the relative phase of the total waves in the forward and backscattering directions. The phase of the total wave in the perpendicular direction is oscillatory, as shown in Fig. 8. The agreement between the present numerical results and those of King and Wu's eigenfunction expansion method is excellent. They are indistinguishable from each other on the graphs shown in Figs. 5-10 for $kr \leq 25$. Eigenfunction expansion solutions for $kr > 25$ are not available for comparison with the present data.

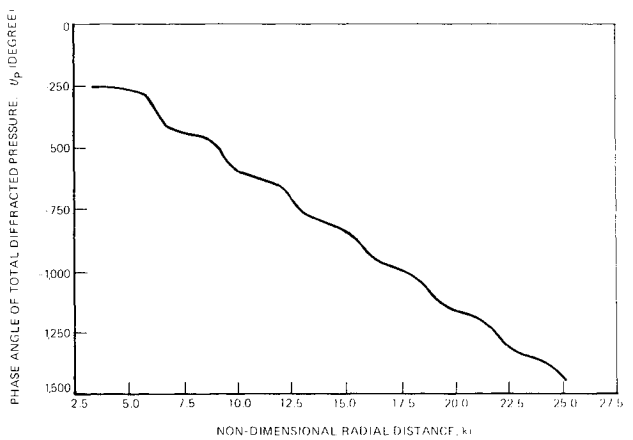

Fig. 10 Phase of total diffracted pressure field; soft cylinder, $ka = 3.1$, $\theta = \pi$.

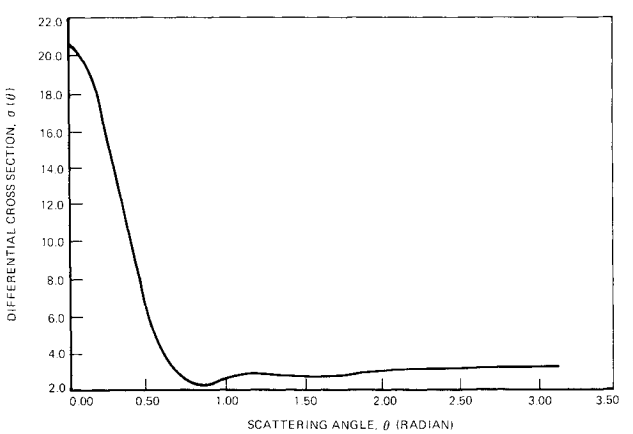

Fig. 11 Distribution of differential cross section in the far field; soft cylinder, $ka = 3.1$

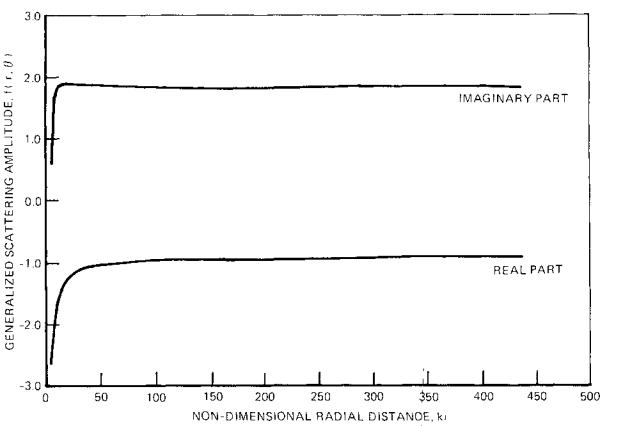

Fig. 12 Generalized scattering amplitude profile; hard cylinder, $ka = 3.1$, $\theta = 0$.

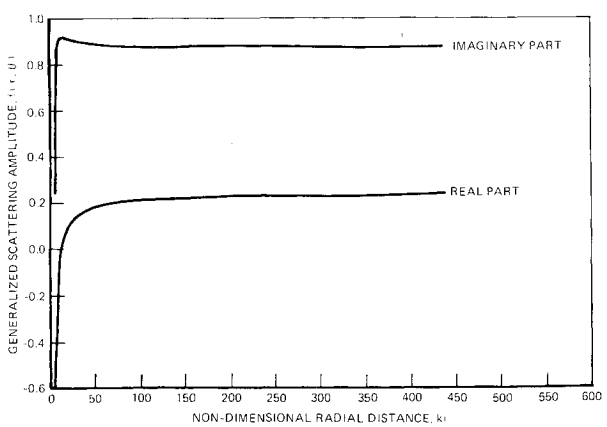

Fig. 13 Generalized scattering amplitude profile; hard cylinder, $ka = 3.1$, $\theta = \pi/2$.

The interference effect can be seen explicitly from the simple expressions for the magnitude of the total wave in the forward, perpendicular, and backscattering directions. In the forward direction, we have $\theta = 0$ and $x = r$. The incident plane wave e^{ikx} coincides with the phase factor e^{ikr} in the scattered wave, and the absolute square of the total wave according to Eq. (6) is given by

$$|\phi|^2 = \frac{(f^i)^2}{kr} + \left(1 + \frac{f^r}{\sqrt{kr}}\right)^2 \tag{20}$$

Since both real and imaginary components of the generalized scattering amplitude in the forward direction are nonoscillatory, as shown in Fig. 2, the amplitude of the total wave should also be nonoscillatory in the forward direction. This is evident in Fig. 5. In the backscattering direction, we have $\theta = \pi$ and $x = -r$. The incident wave e^{ikx} is 180 deg out of phase with the phase factor e^{ikr} in the scattered wave. The absolute square of the total wave becomes

$$|\phi|^2 = \left[1 + \frac{(f^r)^2 + (f^i)^2}{kr}\right] + 2\left[\frac{f^r \cos 2kr - f^i \sin 2kr}{\sqrt{kr}}\right] \tag{21}$$

The second bracketed term on the right-hand side of Eq. (21) causes rapid oscillations in the total wave in the backscattering direction, as shown in Fig. 9. The rapidity of oscillation increases from the forward direction to the backscattering direction. The oscillations in the amplitude of excess pressure, as shown in Fig. 7, are due to the second bracketed term in the following expression for the absolute square of the total wave in the perpendicular direction,

$$|\phi|^2 = \left[1 + \frac{(f^r)^2 + (f^i)^2}{kr}\right] + 2\left[\frac{f^r \cos kr - f^i \sin kr}{\sqrt{kr}}\right] \tag{22}$$

The total wave in the backscattering direction oscillates twice as fast as that in the perpendicular direction. Figure 11 shows the bistatic cross section per unit cylinder length in unit of the cylinder radius as a function of scattering angle for a soft cylinder at $ka = 3.1$. The scattered wave intensity in the far field peaks in the forward direction.

Hard-Cylinder Scattering

For the scattering by a hard cylinder at $ka = 3.1$, the profiles of the generalized scattered amplitude at scattering angles $\theta = 0$, $\pi/2$, and π are shown in Figs. 12–14. As in the soft-cylinder scattering case, these profiles show the existence of a strong interaction region characterized by large gradients in the generalized scattering amplitude near the cylinder's surface. The amplitudes and phases of the total wave computed from the generalized scattering amplitude according to Eq. (6) are in excellent agreement with the eigenfunction expansion solutions given in Ref. 2 for $kr \leq 25$. The profile of the bistatic cross sections per unit cylinder length in unit of the cylinder radius is shown in Fig. 15. The scattered wave intensity in the far field also peaks in the forward direction.

In the case of hard-cylinder scattering, the incident plane wave and the scattered wave exert nonvanishing excess pressures on the cylinder at its surface. The net force on the cylinder is in the direction of the plane wave propagation and can be computed by integrating the complex excess pressure over the cylinder's circumference. Figure 16 shows the amplitude of the sideward force per unit cylinder length divided by cylinder circumference as a function of ka. The data of the present computation are in excellent agreement with those given by Morse[1] for $ka \leq 5$.

The present method has been applied to ka values ranging from 0.1 to 12 for both soft- and hard-cylinder scatterings. The agreement between results of the present study for

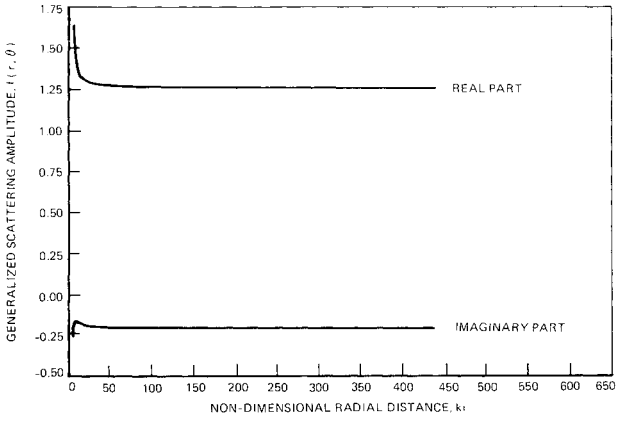

Fig. 14 Generalized scattering amplitude profile; hard cylinder, $ka = 3.1$, $\theta = \pi$.

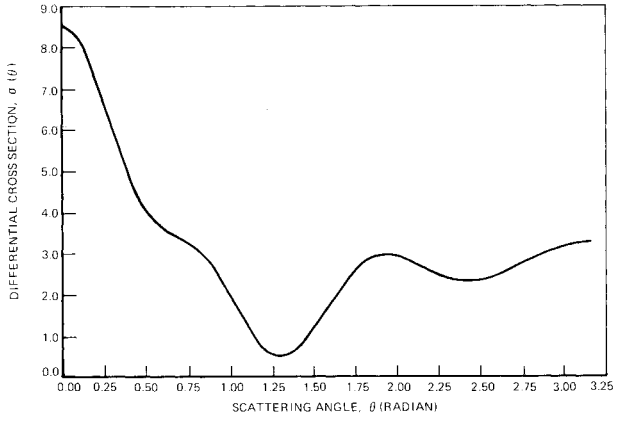

Fig. 15 Distribution of differential cross sections in the far field; hard cylinder, $ka = 3.1$.

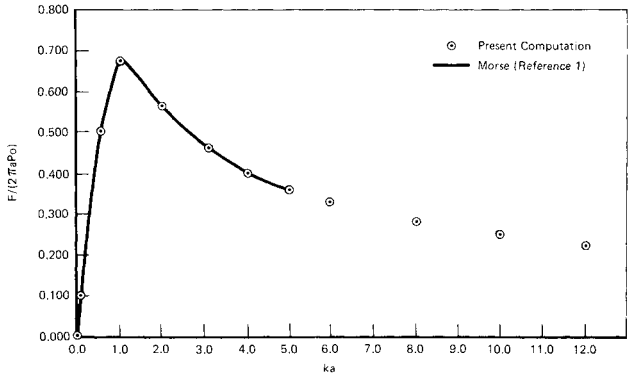

Fig. 16 Amplitude of sideward force per unit length F on a cylinder of radius a. P_0 is the amplitude of incident plane wave.

amplitudes and phases of the induced currents on the cylinder surface and those of the bistatic far-field scattered waves, as given in Ref. 3 for $ka = 1$, 5, and 10, is excellent.

As a further check on the accuracy of the numerical results presented, we employ the optical theorem that relates the total scattering cross section to the forward scattering amplitude. In Table 1, the total scattering cross sections computed from the optical theorem are compared with those obtained by numerical integration of the bistatic cross sections and by the analytic formulas given by King and Wu[2]. The optical theorem is satisfied to within 3% error in most cases. King and Wu's analytic formulas provide accurate total scattering cross sections except at low ka values for hard-cylinder scattering.

Table 1 Total scattering cross section

ka	Soft cylinder			Hard cylinder		
	I	II	III	I	II	III
1.0	5.9129	5.9000	5.9156	2.0104	2.0790	1.7304
2.0	5.2355	5.2061	5.2264	2.7153	2.7843	2.6365
3.1	4.9240	4.8707	4.9222	3.0513	3.1355	3.0231
4.0	4.7909	4.7580	4.7805	3.2073	3.2351	3.1942
5.0	4.6704	4.6263	4.6741	3.3181	3.3821	3.3182
5.97	4.6022	4.5426	4.5998	3.3944	3.4773	3.4023
8.0	4.4722	4.4174	4.4945	3.4569	3.5634	3.5180
10.0	4.4124	4.3215	4.4266	3.5152	3.6454	3.5902
12.0	4.4146	4.2824	4.3781	3.6525	3.7773	3.6407

Note: Method I: Numerical integration of differential cross sections. Method II: Application of optical theorem. Method III: Analytic formula in powers of *ka*.

The soft- and hard-cylinder computations are performed separately because of the different surface boundary conditions. Typical CPU time for a single computation with $ka = 3.1$ and a 77×33 grid network is less than a minute on an IBM 3081 machine.

V. Conclusions

The results presented demonstrate that the finite-difference method for the solution of the transformed Helmholtz equation is an accurate and efficient numerical method for the scattering of sound waves. The unique feature of this approach is the introduction of the nonoscillatory generalized scattering amplitude that characterizes the scattering problems. This introduction makes it possible to apply the finite-difference method to scattering problems in a manner similar to the application of this method to numerical solutions of ordinary fluid dynamics problems. The flexibility of the finite-difference method allows ready generalization for application to complex body shapes, size, and material properties of the scattering obstacle.

Acknowledgments

This work was performed under Northrop's Independent Research and Development Program. The author expresses his appreciation to Mr. M.W. George and Mr. H.A. Gerhardt for managerial support of this study. He also thanks Dr. A.D. Varvatsis for many fruitful technical discussions during the course of the investigation.

References

[1]Morse, P.M., "*Vibration and Sound*," McGraw-Hill, New York, 1948.

[2]King, R.W.P. and Wu, T.T., "*The Scattering and Diffraction of Waves*," Harvard University Press, Cambridge, MA, 1959.

[3]Bowman, J.J., Senior, T.B.A., and Uslenghi, P.L.E., "*Electromagnetic and Acoustic Scattering by Simple Shapes*," North-Holland Publishing Company, Amsterdam, the Netherlands, 1969.

[4]Bayliss, A., Gunzburger, J., and Turkel, E., "Boundary Conditions for the Numerical Solution of Elliptic Equations in Exterior Regions," *Journal of Applied Mathematics*, Vol. 42, April, 1982, pp. 430–451.

[5]Bayliss, A., Goldstein, C.I., and Turkel, E., "An Iterative Method for the Helmholtz Equation," *Journal of Computational Physics*, Vol. 49, March, 1983, pp. 443–457.

[6]Bayliss, A. and Turkel, E., "Far Field Boundary Conditions for Compressible Flows," *Journal of Computational Physics*, Vol. 48, Nov. 1982, pp. 182–199.

[7]Burton, A.J., "Numerical Solution of Scalar Diffraction Problems," *Numerical Solution of Integral Equation*, edited by L.M. L.M. and Walsh, J. Claredon, Oxford, England 1974.

[8]Bayliss, A. and Maestrello, L., "Measurements and Analysis of Far Field Scattering from a Prolate Spheroid," *Journal of the Acoustical Society of America*, Vol. 64, Sept. 1978, pp. 896–900.

[9]Baumeister, K.J., "Finite-Difference Theory for Sound Propagation in a Lined Duct with Uniform Flow Using the Wave Envelope Concept," NASA TP-1001, 1977.

[10]Baumeister, K.J., "Time-Dependent Wave Envelope Finite Difference Analysis of Sound Propagation," *AIAA Journal*, Vol. 24, Jan. 1986, pp. 32–38.